8-2018

Characterization of a Variant of Tuberous Sclerosis Complex 2 and its Interaction with Rheb

Sowmya Sivakumar
University of Arkansas, Fayetteville

Characterization of a Variant of Tuberous Sclerosis Complex 2 and its Interaction with Rheb

A thesis submitted in partial fulfillment
of the requirements for the degree of
Master of Science in Cell and Molecular Biology

by

Sowmya Sivakumar
Hendrix College
Bachelor of Arts in Biochemistry and Molecular Biology

August 2018
University of Arkansas

This thesis is approved for recommendation to the Graduate Council

_____
Paul Adams, Ph. D.
Thesis Director

_____
Colin Heyes, Ph. D.
Committee Member

_____
Suresh Thallapuranam, Ph. D.
Committee Member

_____
Ralph Henry, Ph. D.
Committee Member

ABSTRACT

Protein-protein interactions are vital in maintaining proper function and homeostasis in cells. Some signaling pathways are regulated by G-proteins that work like switches to activate and deactivate pathways. Mutations in these proteins, their effectors or the interaction between proteins may cause dysregulation of signals that can lead to many diseases.

Rheb, Ras homology enriched in brain, is a Ras family GTPase that is vital in regulation of the mTOR (mammalian target of rapamycin) pathway that signals cell proliferation and growth. Due to the low intrinsic GTPase activity of Rheb, a GTPase activating protein (GAP), Tuberous Sclerosis Complex 2 (TSC2) down regulates Rheb by enhancing its GTPase activity. Currently, very little information is available about TSC2 structures and the molecular details of the interaction between the two proteins. We explored various biochemical and biophysical information of Rheb-TSC2 interaction. In addition, we characterized the stability of the variant, TSC2-218 (D74A), using a 218 amino acid truncated construct of TSC2, and the effects of the single point mutation on the interactions with Rheb. In comparison to the WT, the D74A variant showed to maintain protein stability (thermal and chemical), an increase in secondary (alpha helical) structure, binding and GAP activity towards Rheb.

TABLE OF CONTENTS

INDEX

CD	Circular Dichroism
CV	Column Volume
DSC	Differential Scanning Calorimetry
DNAse	Deoxyribonuclease I (Bovine pancreas)
EDTA	Ethylenediaminetetraacetic acid
F_d	Fraction Denatured
F_f	Y-axis final value in plot of denaturation studies
F_i	Y-axis initial value in plot of denaturation studies
FPLC	Fast protein liquid chromatography
GAP	GTPase activating protein
GDP	Guanosine diphosphate
GEF	Guanine nucleotide exchange factor
GMPPNP	Guanosine 5′-[β,γ-imido]triphosphate (GTP analog - non-hydrolyzable)
GST-tag	Glutathione-S-Transferase - tag (affinity chromatography)
GTP	Guanosine triphosphate
GTPase	Protein that hydrolyzes GTP to GDP
His_6-tag	Hexa-histadine - tag (affinity chromatography)
IPTG	Isopropyl-β-D-thiogalactoside
ITC	Isothermal titration calorimetry
LB	Lysogeny Broth
mTOR	mammalian target of rapamycin
NMR	Nuclear magnetic resonance
PBS	Phosphate buffered saline

PDB	Protein Data Bank
P_i	Inorganic phosphate
PMSF	phenylmethylsulfonyl fluoride
Rheb	Ras homology enriched in brain
SDS	Sodium dodecyl sulfate
SDS-PAGE	sodium dodecyl sulfate polyacrylamide gel electrophoresis
TSC	Tuberous sclerosis complex
tsc1, TSC1	*tuberous sclerosis complex 1* (gene), tuberous sclerosis complex 1 (protein)
tsc2, TSC2	*tuberous sclerosis complex 2* (gene), tuberous sclerosis complex 2 (protein)
TSC2-218	Small, truncated 218 amino acid construct of Tuberous sclerosis complex 2, corresponds to residues (1525-1742)
TSC2-218 (D74A)	Small, truncated 218 amino acid construct of Tuberous sclerosis complex 2, corresponds to residues (1525-1742) with an aspartic acid to alanine mutation at position 74 (position 1598 in full-length)
WT	Wild Type

I. Chapter 1: Introduction

1.1 mTOR, Ras, GEF and GAP

Protein-protein interaction and signaling are the basis for many biochemical processes in cells. To maintain proper function of metabolic activity, signaling pathways are often regulated by proteins. Any dysregulation of the pathways can lead to improper downstream activity and disease states.

Ras superfamily of G-proteins are a class of highly conserved GTPases that act as switches in various signaling pathways by cycling nucleotides to activate or deactivate the pathways (1). When the protein is bound to GTP (guanosine triphosphate), the protein is biologically active; whereas, when bound to GDP (guanosine diphosphate), the protein is inactive (1).

GTPases are able to intrinsically hydrolyze GTP (active) to GDP (inactive) + P_i (inorganic phosphate). Therefore, GTPases interact with effectors (guanine exchange factors and GTPase activating proteins) that enable nucleotide cycling and hydrolysis (Figure 1).

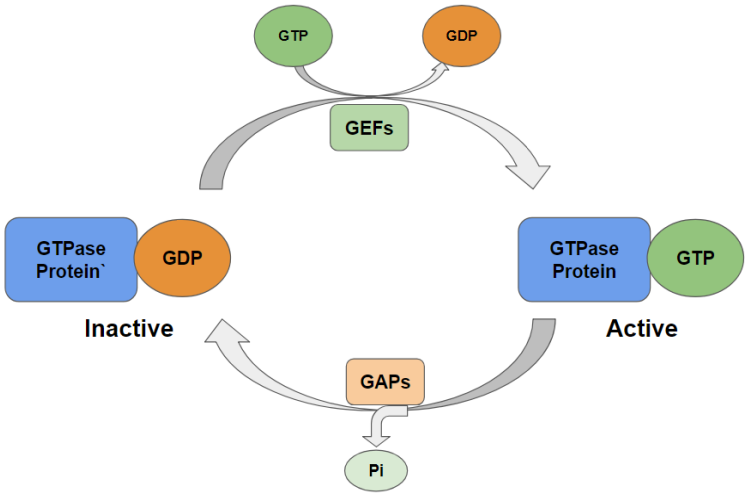

Figure 1**.** Schematic of GTPase protein cycling between active (GTP-bound) and inactive (GDP-bound) states and the roles of guanine exchange factors (GEFs) and GTPase activating proteins (GAPs). Schematic was designed in Google Slides.

Guanine exchange factors (GEFs) bind to GDP-bound GTPase and stimulate the release of GDP, thus allowing the attachment of GTP (found in high concentrations in the cell). This establishes the protein to switch from an inactive to active state and furthers the signal downstream. When the biologically active protein is no longer required, GTP hydrolysis necessary to turn the signal off. This is accomplished by effectors known at GTPase activating proteins (GAPs). GAPs bind to GTPase proteins (GTP-bound and active) and promote GTP hydrolysis to GDP + P_i; thus, the protein is no longer active and the signal downstream is halted.

Small GTPases from the Ras superfamily, specifically Rheb and Rag, are commonly known to regulate mTOR pathway (39). The mTOR, mammalian target of rapamycin, pathway is a vital signaling pathway which regulates cell growth and proliferation by promoting protein, lipids and nucleic acid synthesis (3). mTOR is a serine/threonine kinase that is comprised of 2 functionally different complexes; mTOR complex 1 (mTORC1) and mTOR complex 2 (mTORC2). mTORC1 (referred to as Raptor) is sensitive to rapamycin, whereas, mTORC2 is (referred to as Rictor) is resistant to rapamycin (4) (5) (6). Both mTORC1 and mTORC2 act as scaffolding proteins and they recruit and interact with many regulatory proteins. While mTORC1 functions in protein synthesis via S6K and 4EBP1, mTORC2 centers on phosphorylation of Akt in presence of insulin (7).

Normally, the kinase activity of mTORC1 and mTORC2 towards 4E-BP1 and Akt, respectively, are minimal (7). Active Rheb enhances kinase activity of mTORC1, and thus, increases the amount of phosphorylated 4E-BP1 (substrate of raptor/ mTORC1) in vitro (7) (8). However, Rheb does not augment kinase activity in mTORC2 toward Akt (7) (8). Within the Ras family, Rheb, unlike K-Ras, RalA, RalB and Rad proteins, was the only g-protein to exhibit mTORC1 activation (7). In addition, Rho family small G-proteins were also unable to activate

mTORC1 (7). Due to the importance of the mTOR pathway in maintaining homeostasis, dysregulation of signaling can cause various human diseases such as cancers, obesity, diabetes (9) (10).

1.2 Rheb

Rheb, Ras homology enriched in brain, is a small 20kDa GTPase in the Ras superfamily of GTPases that was first identified in neural tissues primarily in the brain (11).

Many sequences of Rheb are homologous (about 30-45% sequence) with other small GTPases, primarily Ras/Rap subfamily (11). The 5 regions, G1-G5 which are specific to GTP binding, contain the highest homology between Rheb and its corresponding Ras family proteins (11). Structural comparisons also confirm that Rheb is most closely related to the Ras and R family than RhoA and Rab5A (12).

Rheb and other small GTPases have 3 main regions: Switch I (residues 33-41), Switch II (residues 63-79) and P loop, each with distinct characteristics (12) (13) (14). Switch I of small GTPases are vital in identifying and interacting with their effectors; therefore, any variation in primary sequences and/or structures of the Switch I region contributes to the specificity of small GTPases to the corresponding effectors (12). The Switch I sequence of Rheb has high flexibility, like that of other GTPases (most similar to Ras and Rap). Structural comparison of the Switch I region also confirmed higher similarity to Ras and Rap than Rho and Rab, in respect to complexes with nucleotides (GDP, GTP, GTP analog) (12).

The Switch II region displays major differences between small GTPases and Rheb (12). Typically, the Switch II region of small GTPases have an alpha helical conformation when complexed with GTP (or GTP analog), but assume a slightly disordered conformation at the N-terminal when complexed with GDP (15). In the process of GTP and GDP cycling, this Switch II

region undergoes a drastic conformational change in most GTPases. In contrast, in GTP-bound Rheb, the Switch II region is in an unraveled conformation rather than the typical alpha helical conformation as seen in GTPases. Hydrophobic and hydrophilic interactions between key residues in the N-terminal and C-terminal of the Switch II region appear to stabilize the conformation in Rheb (12). Interestingly, Yu *et. al.* found that the Switch II region of Rheb undergoes minimal conformational changes while cycling between GTP and GDP. Also, Switch II residue Gln64 is slightly displaced compared to the corresponding Ras (Gln61) and Rap (Thr61) residues (12). In addition, they found that this polar side chain is positioned away from the GTP-binding site and buried in a hydrophobic pocket (12). This leads to a lack of interaction with GTP, water molecules or nearby catalytic site residues. Further, Ras proteins normally contain a conserved Gly12 in the P loop; in contrast, Rheb has an arginine (R15) and serine (S16) that bind to GDP or GTP (13) (16) (17). The distinct and stable conformormation of Rheb, the inability of residue Gln64 to participate in GTP hydrolysis (unlike Ras counterpart, Gln61) and arginine and serine in lieu of glycine in the P loop, are thought to be the primary reasons for Rheb's low intrinsic GTPase activity.

Data has consistently shown that Rheb has a low intrinsic GTPase activity, which is uncharacteristic of most GTPases, and is found in a constitutively active (GTP-bound) state (18) (19). Therefore, there is a vital need for down regulation of Rheb via protein-protein interaction to prevent consequences of overactive signaling of the mTOR pathway. This is achieved by TSC1-TSC2 complex which acts as a GTPase-activating protein for Rheb and enhances Rheb's ability to undergo GTP hydrolysis in order to return to an inactive GDP-bound state (20) (21) (22) (23) (24).

1.3 TSC2-218

TSC1 and TSC2 (tuberous sclerosis complex 1 and 2) are proteins derived from tsc1 and tsc2 genes (25) (26). These genes were first identified as tumor suppressor genes (27). Mutations found in Tsc1 or Tsc2 genes can cause an autosomal dominant disorder known as tuberous sclerosis (28) (29). This disease state causes various benign tumors (hamartomas) throughout the body and at times, neurological symptoms (28) (29).

TSC1, also referred to as hamartin (140kDa), and TSC2, as tuberin (200kDa), form a heterodimer, known as the tuberous sclerosis complex (TSC) (25) (26). TSC is found in many areas throughout the body including the brain, kidneys, heart, liver, pancreas and other organs (30).

Studies have shown that the GAP domain at the C-terminal of TSC2 is highly conserved and homologous to the Rap1GAP (31) and is able to down-regulate Rheb by enhancing its GTPase activity (28). Specifically, mutations in this TSC2 GAP domain have resulted in a loss of down-regulation of S6K and 4EBP1 (regulatory proteins activated directly by mTORC1) due to loss of Rheb GTPase activity (21) (28). Interestingly, the C-terminus mutations did not affect the interaction of TSC2 with TSC1 and only with Rheb (27). In addition, TSC1 does not seem to alter GTPase activity of Rheb (32). A smaller 400 residue C-terminal construct of TSC2 is unable to bind to TSC1, but still activates GTP hydrolysis in Rheb (32). In 2009, Marshall *et. al,* used an even smaller truncated version of the C-terminal of TSC2 (TSC2-218) to observe the GAP stimulated GTPase activity of Rheb using Real-Time NMR (33). This 218 amino acid truncated version included the GAP domain of TSC2-218 and was still able to maintain GAP activity towards Rheb as depicted in Figure 2A.

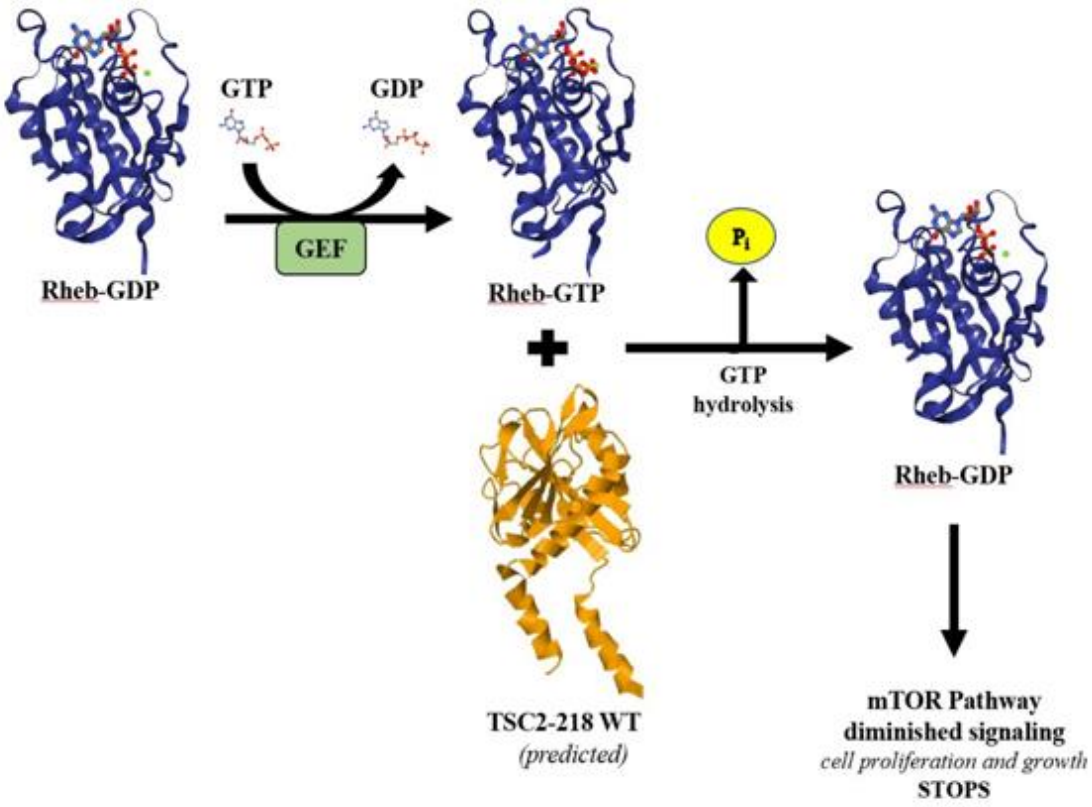

Figure 2A. Schematic of the interaction between TSC2-218 (truncated construct of TSC2) and Rheb and the down stream regulation of mTOR pathway. GTP, GDP, Rheb-GTP (1XTS.pdb) and Rheb-GDP (1XTQ.pdb) structures were obtained through Protein Databank. TSC2-218 WT was predicted using I-TASSER (35) (36) (37) (38). Schematic was made using PowerPoint.

Though Rheb has been studied extensively, there is relatively very little information about its interaction mechanism with TSC2 and the structural characteristics of TSC2. In fact, there is no known full structure of the TSC2 protein. By studying single point mutations in key regions of TSC2, importance of corresponding residues on TSC2 in interactions with Rheb may be better understood.

Marshall and colleagues used Real-Time NMR to observe the distinct structural changes induced by nucleotide dependent conformations to study GTPase activity of Rheb in the presence of TSC2-218 (a 218 amino acid construct from residues 1525 to 1742) and mutations (33). In this study, single point mutations were created in residues that were involved in tuberous sclerosis and residues homologous to Rap1GAP mutations (33).

Most mutations in the TSC2-218 GAP catalytic and binding regions showed similar decrease in GTPase activity as the Rap1GAP homologs, however, there were significant differences in the adjacent and partially conserved regions (28) (33).

The focus of this project will be to study one such mutation (TSC2-218 D74A) that is found in the region adjacent to the catalytic core of TSC2. The corresponding mutation showed an elimination of GAP activity in the homologous RAP1GAP, but not in TSC2 (28) (33). It is possible that the D74A mutation is able to stabilize the interaction with Rheb (unlike other GAP mutations in Ras proteins) and maintain GTPase function of Rheb as suggested in Figure 2B. The truncated 218 amino acid construct of TSC2, TSC2-218, will be used to observe the characteristics of the TSC2 single point mutation, D74A, and its interaction with Rheb.

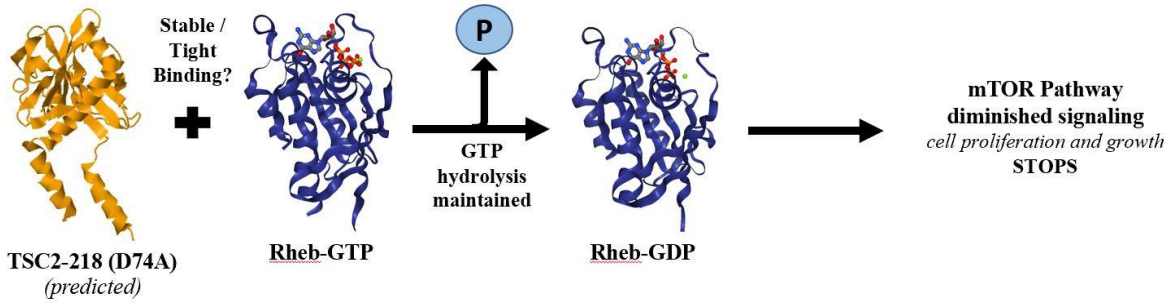

Figure 2B. Schematic of the interaction between TSC2-218 D74A (truncated construct of TSC2) and Rheb and the down stream regulation of mTOR pathway. Rheb-GTP (1XTS.pdb) and Rheb-GDP (1XTQ.pdb) structures were obtained through Protein Databank. TSC2-218 D74A structure was predicted using I-TASSER (35) (36) (37) (38). Schematic was made using PowerPoint

II. Chapter 2: Experimental Methods

2.1 Protein Over-Expression and Purification

2.1.1 Rheb

Ras homology enriched in brain (Rheb) proteins were over-expressed as His_6-tagged (6 histidine residues) fusion proteins and purified using affinity chromatography on a Ni^{2+} column. Rheb was incorporated into the plasmid vector, pET15b, in the *Escherichia coli* (*E. coli*) strain BL21 (DE3) and over-expressed in LB broth. Glycerol stocks were previously made and used in

subsequent over-expression procedures. 1 mL of the pre-existing stocks were added to flasks containing 100mL of LB broth media and 100uL ampicillin and incubated in the shaker at 37°C overnight (between 12 to 16 hours). The next morning, the seed cultures were inoculated into 6L Erlenmeyer flasks containing 1.5L LB broth and 750uL ampicillin and allowed to grow on the shaker at 37°C. The OD (optical density) was measured using a UV-Vis spectrometer at 600nm every hour until the culture reached the target OD of 0.6-0.8. Once in this range, the culture was then induced with 0.5mM IPTG and kept in the shaker at 37°C for four hours. To harvest the cells containing our target protein, each flask was centrifuged at 6,500 rpm for 20min at 4°C. The supernatant was discarded and the pellet was collected and resuspended in 10mM Tris pH 6. The resuspended pellet was then centrifuged at 5,000 rpm for 12-15min at 4°C. The supernatant was discarded and the pellet was stored in -80°C until purification.

Before purification, the pellet was thawed on ice and then resuspended in lysis buffer containing 45mg lysozyme, 150uL halt protease, 1mM PMSF and DNAse. The cells were sonicated on ice for 10 seconds on followed by 10 seconds of rest for a total of 20 minutes. The lysed sample was then centrifuged for 20min at 18,500 rpm at 4°C. The supernatant was collected and subsequently filtered. The sample was then loaded into an FPLC (Fast protein liquid chromatography) machine and purified using affinity chromatography protocols for His6-tagged proteins using a 5ml pre-packed Ni^{2+} column.

PBS Ni^{2+} binding buffer (PBS pH 8.0, 25mM imidazole and 50mM MgCl2) and PBS Ni^{2+} elution (PBS pH 8.0, 400M imidazole and 50mM MgCl2) were made and filtered prior to purification. The 5ml pre-packed Ni^{2+} column was stripped of any residual particles and regenerated with buffers containing nickel. The FPLC machine was washed with autoclaved and filtered water, binding buffer and elution buffer, and the column (attached to the FPLC) was

equilibrated with binding buffer. The protein sample and binding buffer were loaded onto the Ni^{2+} column. The proteins lacking His_6-tag would flow through the column and the target Rheb protein (His_6-tag fusion protein) would bind to the column. Then, increasing amounts of elution buffer were loaded on the column and at approximately 245-250mM imidazole concentration, Rheb would elute. Rheb samples were collected in fractions according to the presence of peaks on the chromatogram. The fractions were collected and band size and purity were confirmed using SDS-PAGE (sodium dodecyl sulfate polyacrylamide gel electrophoresis). The band size was confirmed against a molecular weight ladder and purity was established by lack of appearance of other bands on the gel (Figure 3), the protein sample was dialyzed in Tris pH 8.0 at 4°C overnight (12-16 hours).

If the experiment required Rheb to be active, but unable to undergo intrinsic GTPase hydrolysis, then the sample was subjected to nucleotide exchange in which a nonhydrolyzable GTP analog (GMPPNP) was attached. In this procedure, Rheb was incubated for 1 hour at 4°C with 5mM GTP analog and 5mM EDTA. A desalting column (PD-10) was equilibrated with 5 column volumes of Tris buffer prior to loading the protein sample. Fraction were collected and tested with Bradford assay reagent to determine the presence of proteins. The target fractions were then collected combined and 10mM $MgCl_2$ was added. Purified, and if required, nucleotide exchanged, Rheb protein samples were either immediately stored in -80°C freezer or lyophilized prior to storage (for longer term storage).

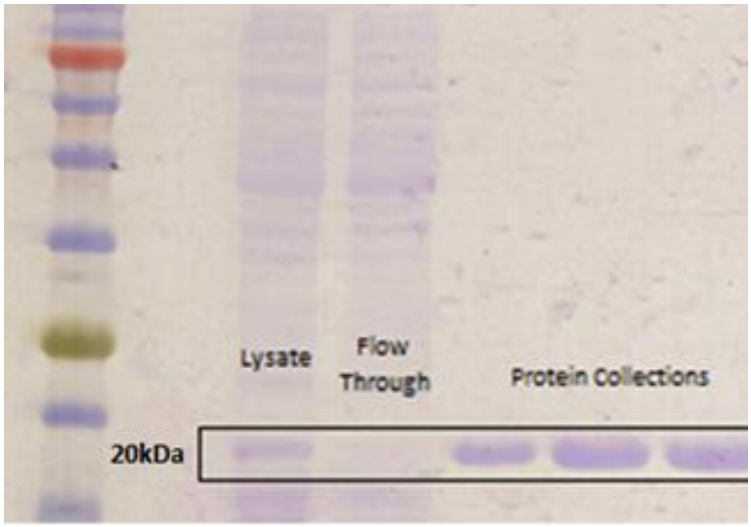

Figure 3. SDS-PAGE (sodium dodecyl sulfate polyacrylamide gel electrophoresis) of a sample purification of His_6-tagged fusion protein, Rheb. The lysate contains all proteins expressed in *E. coli* cell, the flow through contains all proteins that do not bind to Nickel column. When loaded on the column, target His_6-tagged protein, Rheb, will bind and at imidazole concentration of about 250mM, Rheb starts to elute. The fractions containing Rheb are collected. This gel confirms the size of the protein to be around 20 kDa which corresponds to the molecular weight of Rheb. In addition, there is a lack of additional bands seen in the gel which confirms the relative purity of the purified protein sample.

2.1.2 TSC2-218 (WT)

Tuberous sclerosis complex 2 construct with 218 amino acids (TSC2-218) proteins were GST-tagged fusion protein (contain glutathione-S-transferase tag at the N-terminus), over-expressed and purified using affinity chromatography on a GST affinity column. GST-TSC2-218 was incorporated into the plasmid vector, pET15b, in the *Escherichia coli* (*E. coli*) strain BL21 (DE3) and over-expressed in LB broth. Glycerol stocks were previously made and used in subsequent growth/harvesting procedures similar to that of the Rheb listed above. Unlike for Rheb, TSC2-218 proteins were allowed to grow until reaching an OD_{600} of 0.9-1.0 before induction by 0.5mM IPTG, followed by 4.5 to 5 hours incubation in 37°C. Cells were harvested similarly to Rheb by centrifugation at 6,500rm for 20min at 4°C and the pellet was resuspended in 10mM Tris pH 6. The resuspended pellet was then centrifuged at 5,000 rpm for 12-15min at 4°C and stored in -80°C until purification.

Before purification, the pellet was thawed on ice and then resuspended in lysis buffer containing 45mg lysozyme, 150uL halt protease, 75ul PMSF and DNAse. The cells were sonicated, centrifuged and filtered in a similar fashion to Rheb. The sample was then loaded into an FPLC (Fast protein liquid chromatography) machine and purified using affinity chromatography protocols for GST-tagged proteins using a 5ml pre-packed GST affinity column.

Binding buffer containing 10mM PBS pH 7.4 and elution buffer containing 0.02mM Tris HCL and 10mM glutathione pH 8.0 (freshly prepared before each purification) were made and filtered prior to purification. The 5ml pre-packed GST affinity column was stripped using 6M guanidine hydrochloride, washed with water, regenerated with two rounds of 30-50ml of buffers 1 (01M Tris and 0.5 M NaCl pH 8.5) and 2 (0.1 M sodium acetate and 0.5 M NaCl pH 4.5), and washed again with water. The FPLC machine lines were washed with water, binding and elution buffer, and the GST affinity column was equilibrated with binding buffer. The protein sample and binding buffer was loaded onto the GST affinity column where the GST tagged fusion protein (TSC2-218) would bind to the column (containing glutathione) and other proteins would flow through the column. When elution buffer prepared with 10mM glutathione, the protein would elute out in fractions that were then collected to be confirmed using SDS-PAGE (Figure 4A). The sample was then dialyzed in PBS pH 7.4 at 4°C overnight (12-16 hours).

The next day, GST-tagged fusion protein, TSC2-218, underwent thrombin cleavage to cleave the GST tag (large, around 26kDa) from the protein. One unit of thrombin was added for every 100µg of protein and incubated for 1-2 hours at 4°C. About 75µl Halt protease inhibitor cocktail was then added to the mixture and the sample underwent a subsequent purification in order to remove GST from the protein sample. This purification is similar in procedure, however, the free GST binds to the column and the unbound/properly cleaved target protein (TSC2-218)

flows through the column and is collected in fractions. The samples are then checked via SDS-PAGE (Figure 4B) and dialyzed using PBS buffer pH 7.4 then subsequently stored at -80°C.

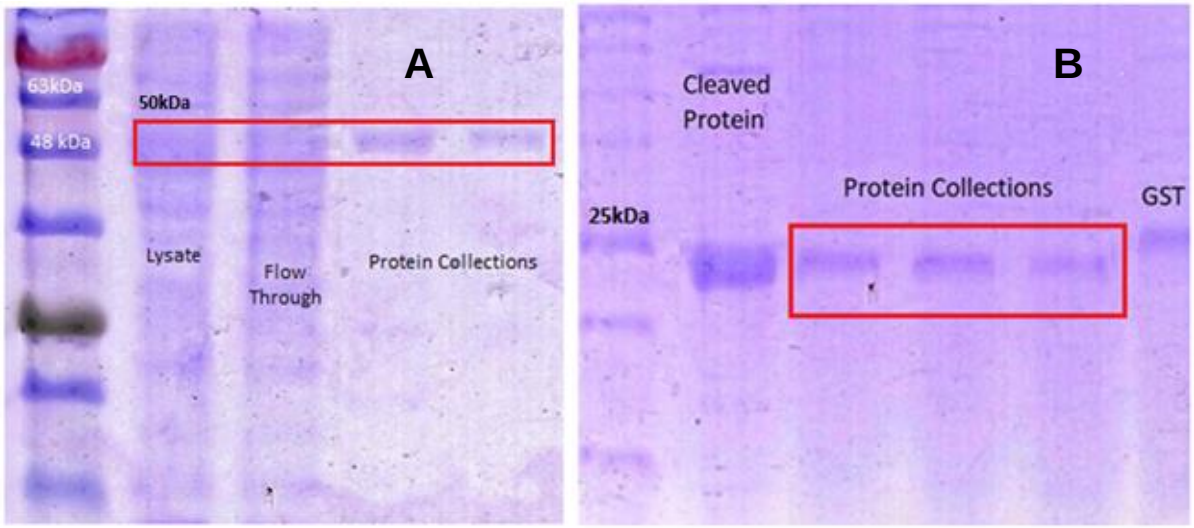

Figure 4. SDS-PAGE gels of GST-TSC2-218 samples from the GST-fusion protein purification (A) and subsequent TSC2-218, target protein, purification (B). (A) Lane 1 contains molecular weight ladder, Lysate contains all proteins expressed by cell, Flow through contains proteins lacking the GST affinity tag. GST-TSC2-218 elutes with addition of Elution buffer (Glutathione concentration of 10mM) and fractions containing protein was collected (Protein Collections). (B) Cleaved protein includes all proteins after thrombin cleavage. Target TSC2-218 protein flows through the column and is collected. With the addition of elution buffer containing 10mM glutathione, GST elutes. Bands are checked on SDS-gel for size and purity.

2.1.3 TSC2-218 (D74A)

The procedure for the variant of TSC2-218, D74A, was almost identical to the wild-type. However, since there were no glycerol stocks of the variant available, plasmids for TSC2-218 (D74A) were acquired and transformed with *E. coli* NEB 5-alpha strain for plasmid amplification. After transformation, the cells were plated in LB agar and allowed to grow overnight at 37°C. Plasmids were isolated from the culture and sequenced (at UAMS DNA Sequencing Laboratory in Department of Microbiology and Immunology) to check for correct genetic sequence. After confirmation the sequencing, plasmids were then transformed into *E. coli* BL21 (DE3) cells for over-expression.

Test expressions were performed on the over-expression of *E. coli* cells containing GST-TSC2-218 (D74A) to optimize conditions to achieve best yields. Conditions that were specifically tested were the optimal OD_{600} range and amount of IPTG to induce cell cultures. 1ml of glycerol stocks were incubated in the shaker at 37°C in 10mL LB media in a 50m falcon tube with 10uL ampicillin overnight (12-16 hours). The next day, the 10ml cultures were added to a 500ml Erlenmeyer flask containing 90ml LB media, 100uL ampicillin and incubated in the shaker at 37°C. OD_{600} (optical density at 600nm) readings were taken on the UV-Vis spectrometer every 15 min and recorded. Using Excel, the data was converted into a graph (Figure 5). The mid log phase was determined to be at around OD_{600} = 0.8-1.0. This was determined to be the optimal OD range (which was similar to the wild-type).

To confirm the proper absorbance and determine the optimal concentration of IPTG needed to induce higher yield of protein, 1 ml was taken from each sample at OD = 0.4, 0.6, 0.8 and 1.0 and incubated with 0.5mM and 1.0mM IPTG and incubated in the shaker at 37°C for 4 hours. Each 1ml sample was prepared for SDS-PAGE by being centrifuged at 13,000 rpm for 3 minutes, the supernatant was removed, 15uL of 2X sample dye was added and the sample was heated for 5 minutes at 80°C. After 4 hours, another 1mL of each sample was placed into a 2ml centrifuge tube and the steps for sample preparation were repeated. The pre-induction, post induction and molecular ladder samples were all loaded onto a 15% polyacrylamide gels and SDS-PAGE was performed (Figure 6A). Band intensities were quantified using densitometry analysis using UN-SCAN- IT. As represented in Figure 6B, the values were then graphed using Excel. It was determined that the optimal OD range was around 1.00 and the 1mM IPTG was only yielded slightly higher band intensity than the 0.5mM so 0.5mM IPTG was used in subsequent inductions.

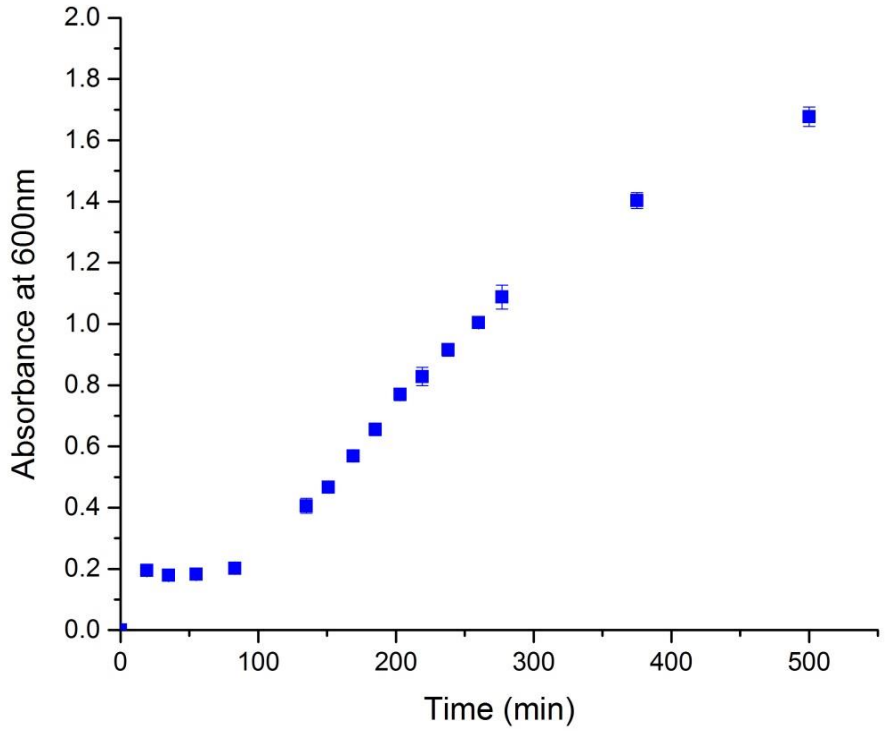

Figure 5: Test expression for optimal optical density range (A600nm). An absorbance was measured every 15 minutes after inoculation. The data was then recorded and graphically presented with the use of Excel. The test expression was performed in triplicate.

Lane 1: MW Ladder
Lane 2: OD 0.4 - Pre-Induction
Lane 3: OD 0.4 - 0.5M IPTG
Lane 4: OD 0.4 - 1.0M IPTG
Lane 5: OD 0.6 - Pre-Induction
Lane 6: OD 0.6 - 0.5M IPTG
Lane 7: OD 0.6 - 1.0M IPTG
Lane 8: OD 0.8 - Pre-Induction
Lane 9: OD 0.8 - 0.5M IPTG
Lane 10: OD 0.8 - 1.0M IPTG
Lane 11: OD 1.0 - Pre-Induction
Lane 12: OD 1.0 - 0.5M IPTG
Lane 13: OD 1.0 - 1.0M IPTG

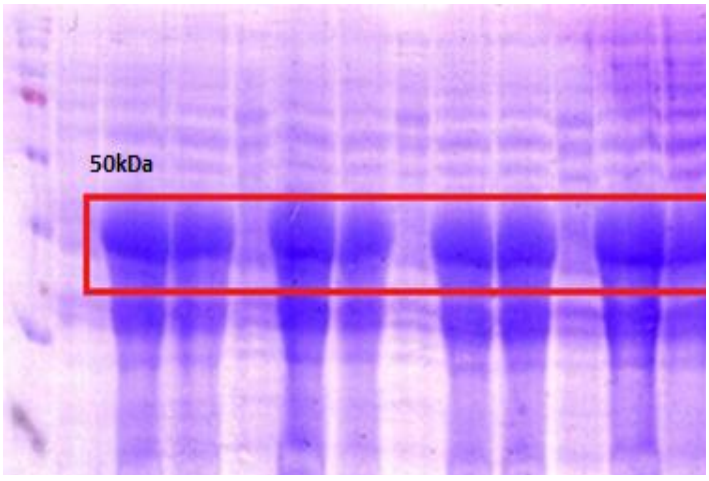

Figure 6A. Test expression for optimal OD and IPTG amount. Pre-induction and post-induction samples were collected, centrifuged, resuspended in sample dye and loaded onto a 15% polyacrylamide gel.

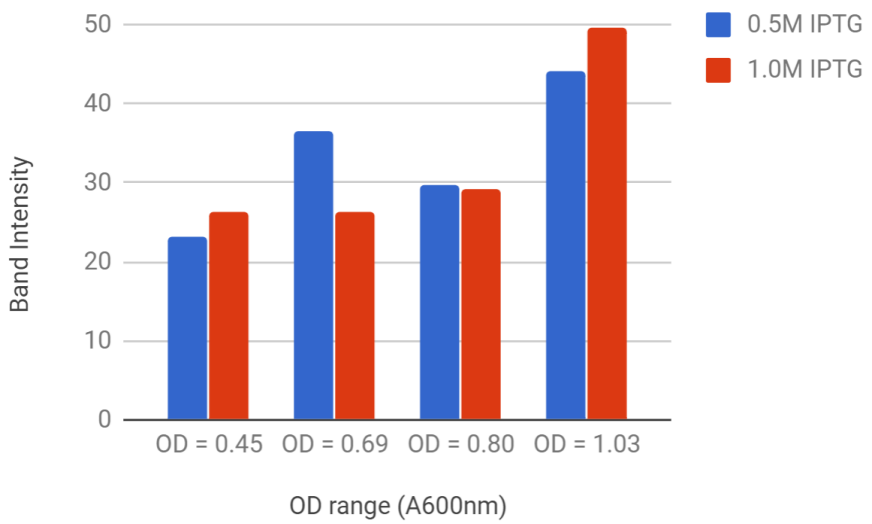

Figure 6B: Graphical representation of densitometric analysis of test expression for optimal optical density and IPTG concentration. Excel was employed to create this graph.

2.2 Characterization Studies of TSC2-218 (WT) and TSC2-218 (D74A)

2.2.1 Circular Dichroism Spectra

JASCO Corp., J-1500 Spectrometer was used to take circular dichroism measurements of purified protein samples of TSC2-218 (WT and D74A) in the far-UV range (190-250nm) using a 2mm pathlength Starna Cells quartz cuvette (Catalog Number: 3-Q-10). The protein concentration of the samples was diluted to 0.2mg/ml in 10mM phosphate buffer pH of 7.4). The spectra were measured at 50nm/min for each sample. A spectrum of a cell containing only buffer was recorded and subtracted from each sample measurement using Excel. Graphs of CD spectra measurements were obtained using Spectra Manager.

2.2.2 Urea Denaturation

Urea denaturation experiments were carried out using the JASCO Corp., J-1500 Spectrometer in 300nm to 400nm range using 10mm pathlength Starna Cells quartz cuvette (Catalog Number: 9-Q-10). The purified samples of TSC2-218 (WT and D74A) were diluted to 0.2mg/ml in 10mM phosphate buffer pH of 7.4. A total of 14 spectra were recorded over an

increasing concentration of 8 Molar (M) urea in autoclaved and filtered water. Urea was titrated using the Automatic Titration Scan measurement program from a range of 0M to 6.4M urea at 25°C. A baseline buffer spectrum was subtracted from each spectrum using Excel and this experiment was 2-3 times for each construct of TSC2-218.

To determine the ratio of unfolded protein (F_d) vs concentration of urea, the following equation (Equation 1) was used where F_i, F_f and F represent initial (native state) intensity, final intensity and intensity at each point of urea denaturation (34).

$$F_d = \frac{(F - F_i)}{(F_f - F_i)} \qquad \text{(Eq. 1)}$$

2.2.3 Thermal Denaturation

Thermal denaturation studies were carried out using JASCO Corp., J-1500 Spectrometer in the far UV CD (190nm-250nm) using 10nm pathlength Starna Cells quartz cuvette (Catalog Number: 3-Q-10). The purified samples of TSC2-218 (wild type and D74A) were diluted to 0.28mg/ml in 10mM phosphate buffer pH of 7.4. A total of 14 spectra were recorded with increasing temperature from 25°C to 90°C. A baseline buffer spectrum was subtracted from each spectral value using Excel. This experiment was performed with 2-3 samples each and the data averaged for both TSC2-218 wild type and variant (D74A) samples. Excel was employed to calculate the ratio of unfolded protein versus temperature for each of the samples and graphically presented.

2.3 Interaction Studies between RHEB and TSC2-218 (WT and D74A)

2.3.1 Circular Dichroism Difference Spectra

CD difference spectra measurements were also performed using JASCO Corp., J-1500 Spectrometer in the far-UV CD range (190-250nm). The purified protein (Rheb) and effector protein (TSC2-218) samples were diluted to concentrations of 0.2mg/ml in 10mM phosphate

buffer pH of 7.4, to maintain a ratio of 1:1. CD measurements of each sample were taken prior to incubation. Protein and ligand samples were then incubated together for 30 min at 4°C and CD measurements were gathered at 0 min and 30 min after incubation. The spectra were measured at 50nm/min for each sample. A buffer spectrum was collected and subtracted from each sample spectra using Excel. TSC2-218 spectra were then subtracted from the mixture spectra using Excel and graphs of difference spectra were obtained using Spectra Manager and Excel.

2.3.2 GTPase Hydrolysis Assay

GTP hydrolysis assays were carried out using GTPase-Glo Assay Kit (Promega V7681) and white 384 Well Polystyrene Microplates (Greiner Bio-One Catalog # 781075) in order to observe differences in GTPase Activity in Rheb in the presence and absence of TSC2-218 (WT and D74A). After purification of the Ras GTPase (Rheb), nucleotide exchange with the nonhydrolyzable GTP analog was not performed. All samples of Rheb and its GAP effectors, TSC2-218 (WT and D74A), were dialyzed in PBS (pH 7.4) and samples were run on the gel to confirm the presence of protein prior to performing experiments. The protein samples were diluted in GTPase/GAP buffer (provided in kit) and luminescence was recorded using the BioTek Gen5 program and Synergy H1 Hybrid plate reader. The relationship between GTP concentration and luminescence is provided in Figure 7, where luminescence represents the GTP concentration.

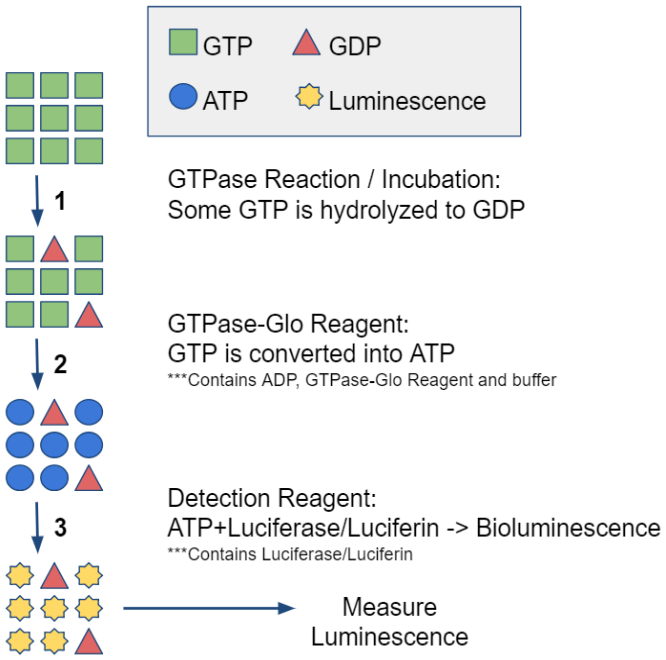

Figure 7. Schematic of Promega GTPase Activity Assay describing the procedure summary of GTPase reaction, incubation, and addition of Reagent 1 (GTPase-Glo Reagent) and Reagent 2 (Detection Reagent).

To observe Rheb's intrinsic GTP hydrolysis activity, 5uL of Rheb (at various concentrations from 0uM to 4uM) and 1mM DTT was incubated for 90min at room temperature with 5uL of 10uM GTP (in GAP buffer). Then, 10uL of reconstituted Glo-GTPase Reagent (freshly made 15 min prior to use) was added to each reaction and incubated shaking at room temperature for 30min. Then, 20uL of detection reagent (provided in kit) was added to each well and incubated at room temperature for 5-10min and luminescence was recorded using Gen5 program on the plate reader. The data was then exported to Excel and Origin and graphically presented

Once the variables were optimized in multiple test experiments, GTPase Activity Assay was performed on 10µM Rheb (with 10mM Mg added) in the presence and absence of 2.25µM TSC2-218 WT and D74A in the following method, where Solutions 1 and 2 were prepared separately for each sample and then added to the wells to initiate the reaction (Table 2).

Table 2. Contents of the solution for each variable in the GTPase activity assay. Solution one was added to the wells first and then solution 2 was added to start the GTPase reaction.

	Solution 1	Solution 2
GTP Only	1mM DTT in GTPase/GAP buffer	10uM GTP in GTPase/GAP buffer
Rheb Only	10uM Rheb and 1mM DTT	10uM GTP in GTPase/GAP buffer
Rheb + WT	10uM Rheb and 1mM DTT in GTPase/GAP buffer	2.25uM TSC2-218 (WT) and 10uM GTP in GTPase/GAP buffer
Rheb + D74A	10uM Rheb and 1mM DTT in GTPase/GAP buffer	2.25uM TSC2-218 (WT) and 10uM GTP in GTPase/GAP buffer

GAP concentration dependent studies were also performed using TSC2-218 (WT and D74A) concentrations from 0uM to 2.1uM in the presence of 10uM Rheb. The 0uM TSC2-218 group represented the Rheb control group as it included only Rheb, GTP and all other buffers (and no GAP protein). A 10uM GTP only group was also tested and this luminescence value was used to represent the total GTP concentration in the solution. This experiment was repeated 2-4 times for each sample.

III. Chapter 3: Results

3.1 Characterization Studies of TSC2-218 (WT) and TSC2-218 (D74A)

3.1.1 Circular Dichroism Spectra

To observe the characteristic differences between TSC2-218 Wild-type and variant (D74A), experiments focusing on the structural, chemical and physical properties were performed.

The secondary structural differences were compared by performing circular dichroism studies on TSC2-218 wild-type and variant (D74A). The CD spectra for the variant of TSC2-218, D74A, is similar to that of wild-type (WT) (Figure 8). Specifically, there are noticeable negative peaks at approximately 208 and 223nm which correspond to those of standard alpha helix spectra (208 and 222nm).

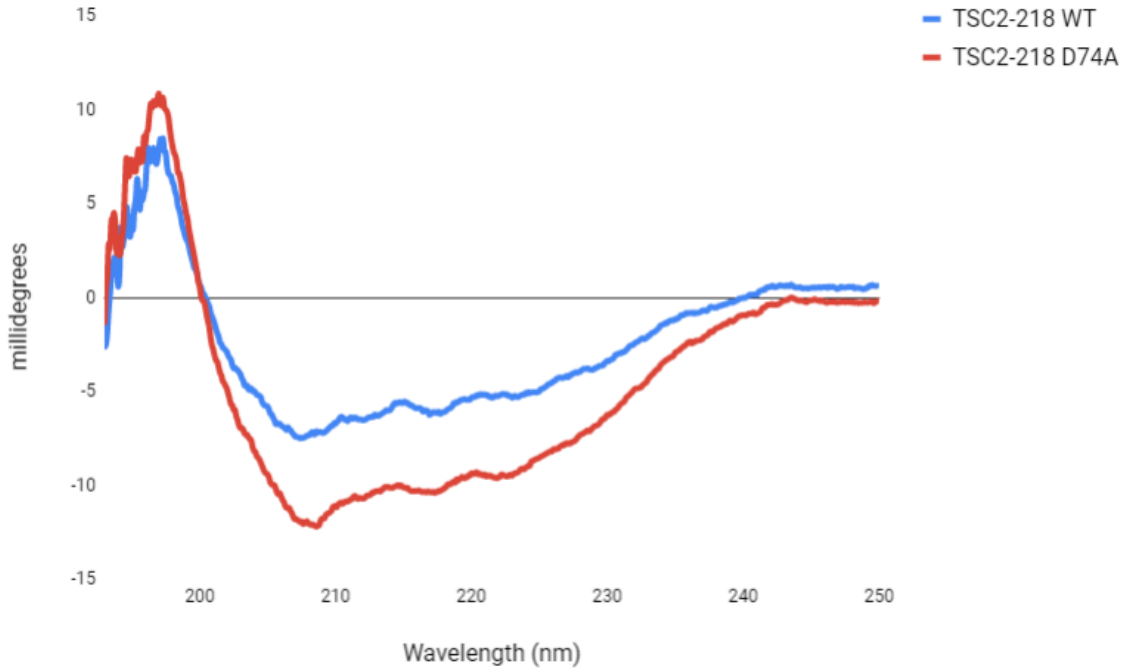

Figure 8: Circular Dichroism (CD) Spectra of TSC2-218 Wild Type (WT) and variant (D74A). Jasco Spectral Management was used to obtain CD spectra data and Excel was used to graphically present the molar ellipticity data for TSC2-218 wild-type and variant.

3.1.2 Urea Denaturation

To assess the protein stability of the TSC2-218 (D74A) in comparison to wild-type, urea denaturation experiments were performed. The presence of urea, a chemical denaturant, disrupts hydrogen bonding (found in secondary and tertiary structure of proteins) and in turn induces the protein to unravel. Thus, by increasing urea concentrations, the protein begins to unfold. This unfolding causes any hydrophobic tryptophan residues (intrinsic fluorophore) to be exposed which in turn show an increase in fluorescence intensity. TSC2-218 contains 2 tryptophan residues that act as intrinsic fluorophores. With increasing amounts of 8M urea being titrated into the protein samples, both TSC2-218 wild type and variant started to unfold. A raw data of the fluorescence spectra at 0M urea and 6.6M urea show a decrease in fluorescence, in addition to a shift from emission max at approximately 338-340nm to 348nm, respectively (Figure 9A).

Looking at Figure 9B (fraction denatured over urea concentration), initially (at low urea concentrations) the amount of unfolded protein of both WT and D74A slowly increases, then the protein sample contains mostly unfolded protein with a urea concentration of around 6.6M. Comparison of the averaged WT with the averaged values for the variant (D74A) shows an almost identical graph of protein unfolding (Figure 9B). However, since the urea denaturation plot does not seem to be completely denatured, the Y value from the fitted line in Figure 9B was used as the F_f value for Equation 1. All F_d values were re-adjusted to represent a more accurate fraction denatured versus urea concentration plot (Figure 9C). C_m values (the urea concentration at which half the protein is in an unfolded state and half is in the folded state) were calculated using the adjusted plot. Both TSC2-218 Wild-type and D74A both showed similar values for C_m (3.47M and 3.58M, respectively).

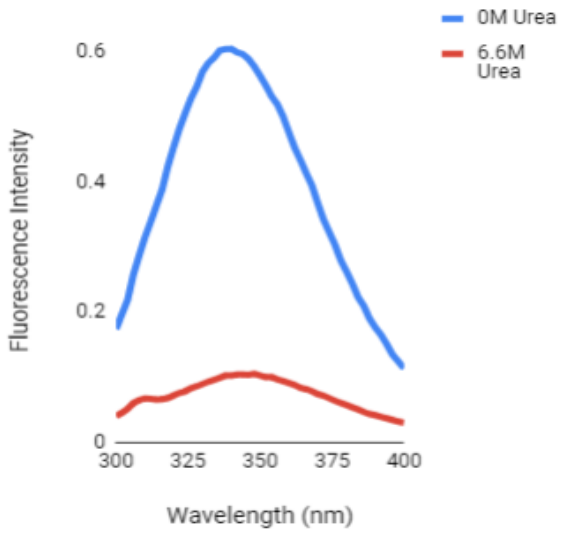

Figure 9A. Fluorescence spectra of TSC2-218 at native (0M Urea) and unfolded (6.6M Urea). There is a distinct decrease in fluorescence at 6.6M urea and a shift from max emission intensity at 338nm at native state and shift towards the right to 348nm for unfolded protein. Data was graphically presented on Origin.

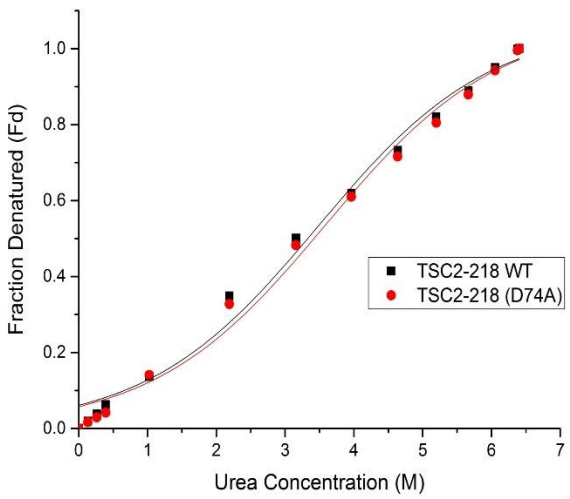

Figure 9B. Fraction denatured (F_d) plot of TSC2-218 Wild-Type (WT) and variant (D74A) against urea concentration (M) using Equation 1. A total of 3 different samples were averaged each for TSC2-218 wild-type and variant using Excel and graphically presented above using Origin.

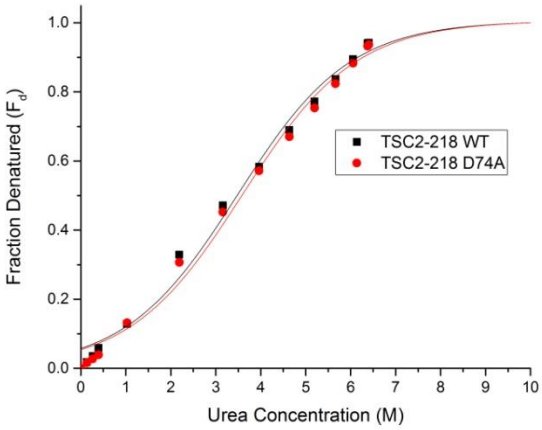

Figure 9C. Urea Denaturation study data representing the adjusted ratio of denatured TSC2-218 WT and variant (D74A) against the urea concentration (M) using Equation 1. F_d values were adjusted using the fitted value at 10M urea from Figure 9B. C_m values were then derived from this adjusted plot. 3 different samples were averaged each for TSC2-218 wild-type and variant using Excel and graphically presented using Origin.

3.1.3 Thermal Denaturation

Thermal denaturation studies can help assess the protein's thermal stability, indirectly. As temperature increases, the protein denatures and begins to unfold due to the disruption of hydrogen bonds forming the secondary structure. As it unfolds, the protein will start to lose its secondary structure characteristics and can be observed using circular dichroism (CD). A thermal denaturation study will aid in determining if the protein stability varies due to an addition of a mutation (TSC2-218 (D74A)). As seen in Figure 10A, as the temperature increases, the fraction unfolded starts to increase. This represents a decrease in secondary structure. Thus, when looking at the ratio of folded to unfolded protein, the protein continues to unfold with increasing temperature until about 85°C when the protein seems to be mostly unfold (Figure 10A). Comparison of the averaged WT with the averaged values for the variant shows a very similar graph of protein unfolding (Figure 10A). However, the proteins were not completely unfolded/denatured. Therefore, the raw data for TSC2-218 WT and D74A spectra was graphed and fitted using Origin (Figure 10B). The value from the fitted line at temperature of 150°C

(where the protein is suggested to be completely unfolded/denatured) was used as the F_f value in Equation 1 in order to adjust the data to a more accurate fraction denatured plot. All measured values were then adjusted and F_d was plotted against temperature (Figure 10C). The T_m, temperature at which the F_d value is 0.5 (half unfolded), values for TSC2-218 WT and D74A were 69.55°C and 70.80°C, respectively.

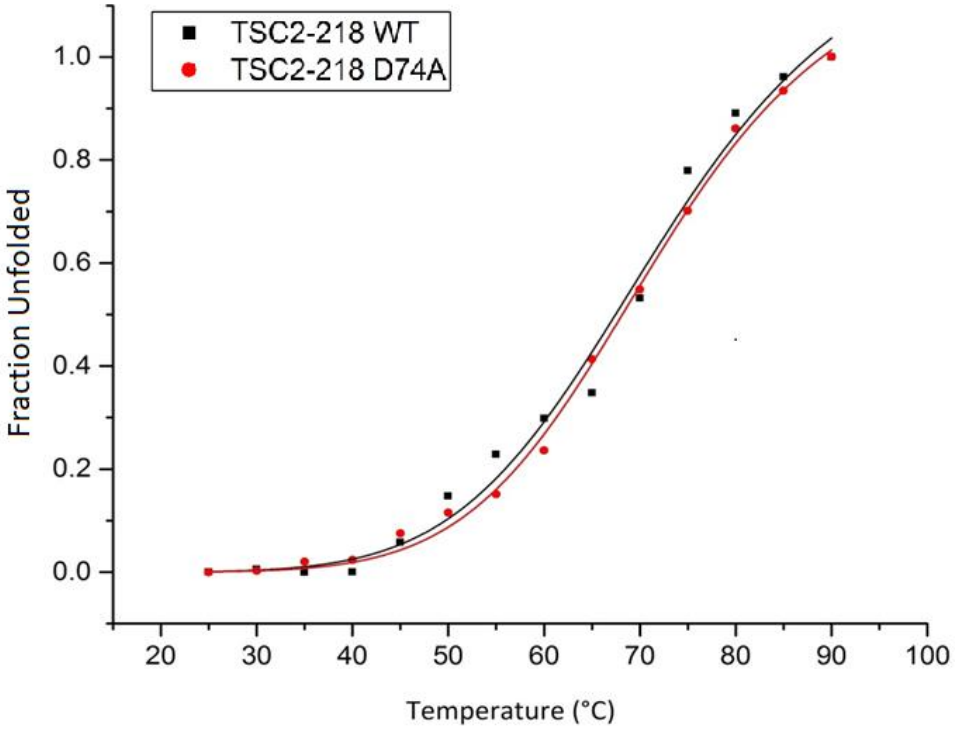

Figure 10A: Thermal Denaturation study data representing the ratio of denatured TSC2-218 Wild-Type (WT) and variant (D74A) against the temperature (°C) using Equation 1. A total of 2-3 different samples were averaged each for TSC2-218 wild-type and variant using Excel and graphically presented using Origin.

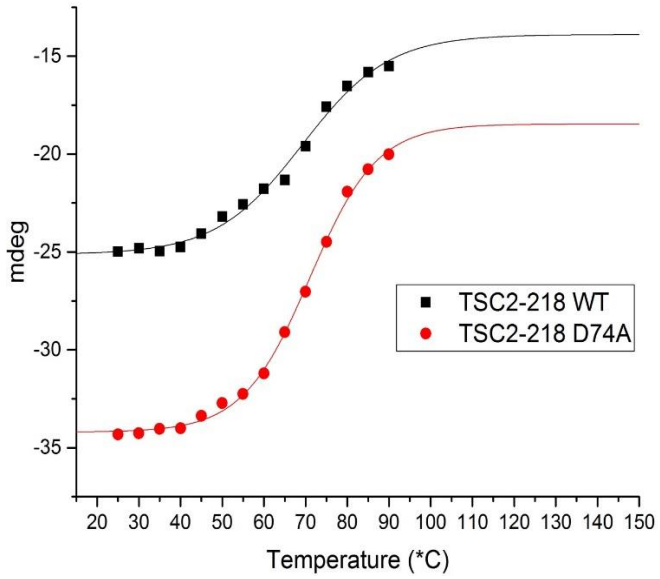

Figure 10B: Raw averaged thermal denaturation data representing the adjusted ratio of denatured TSC2-218 Wild-Type (WT) and variant (D74A) against the temperature (°C) using Equation 1. In addition, F_d values were normalized to extrapolated data values at temperatures of 120, 130, 140 and 150°C (obtained from fitted line from Figure 10B). A total of 2-3 different samples were averaged each for TSC2-218 wild-type and variant using Excel and graphically presented using Origin.

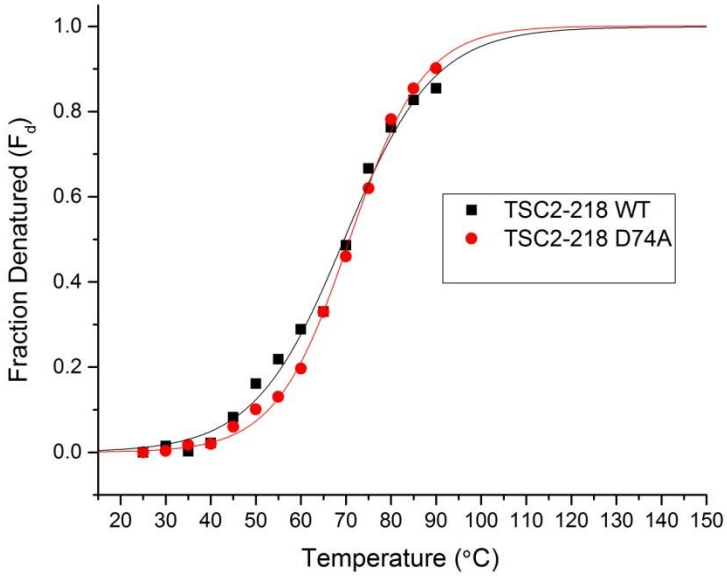

Figure 10C: Thermal Denaturation study data representing the adjusted ratio of denatured TSC2-218 Wild-Type (WT) and variant (D74A) against the temperature (°C) using Equation 1. In addition, F_d were normalized to extrapolated data values at temperatures of 120, 130, 140 and 150°C (obtained from fitted line from Figure 10B). A total of 2-3 different samples were averaged each for TSC2-218 wild-type and variant using Excel and graphically presented using Origin.

3.2 Interaction Studies between RHEB and TSC2-218 (WT and D74A)

3.2.1 Circular Dichroism Difference Spectra

Circular dichroism (CD) difference spectra were used to observe the changes to the structure of Rheb in the presence and absence of TSC2-2128 WT and D74A. If binding is present between two proteins, it can be observed by the change in secondary structure due to a conformational change upon binding. A CD spectrum was measured for each sample of Rheb (Blue line) and TSC2-218, WT and D74A (not present), then the proteins were incubated together and the spectra of the mixture was measured at 0 min and 30 min (Red line). The spectra of the TSC2-218 (WT and D74A) was mathematically subtracted from the mixture (Rheb and TSC2-218) to represent the structural characteristic of Rheb after incubation and possible interaction with TSC2-218 (Orange line). The change in circular dichroism spectra between Rheb (Blue line) and mathematically determined Rheb (Orange line) represents a conformational change. In both Figure 11A and Figure 11B, there is a difference in CD Spectra between Rheb and Corrected Rheb ((Rheb+TSC2-218 Mix spectra) – (TSC2-218 spectra)); therefore, both TSC2-218 wild-type and variant (D74A) exhibit conformational changes due to binding.

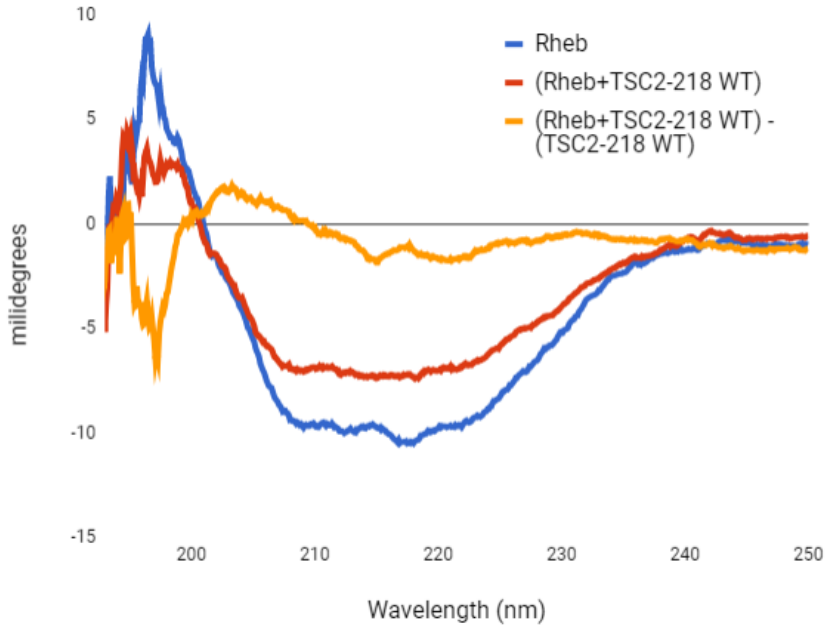

Figure 11A: Circular dichroism (CD) difference spectral data for Rheb in the presence and absence of TSC2-218 wild type (WT) was obtained using Jasco Spectra Measurement program. The data for wavelength vs CD intensity (millidegrees) of Rheb, TSC2-218 WT and Rheb incubated with TSC2-218 WT for 30min was exported and graphically presented using Excel. CD data for WT was then mathematically subtracted from incubated Rheb + TSC2-218 WT mixture to represent the Corrected Rheb CD spectra.

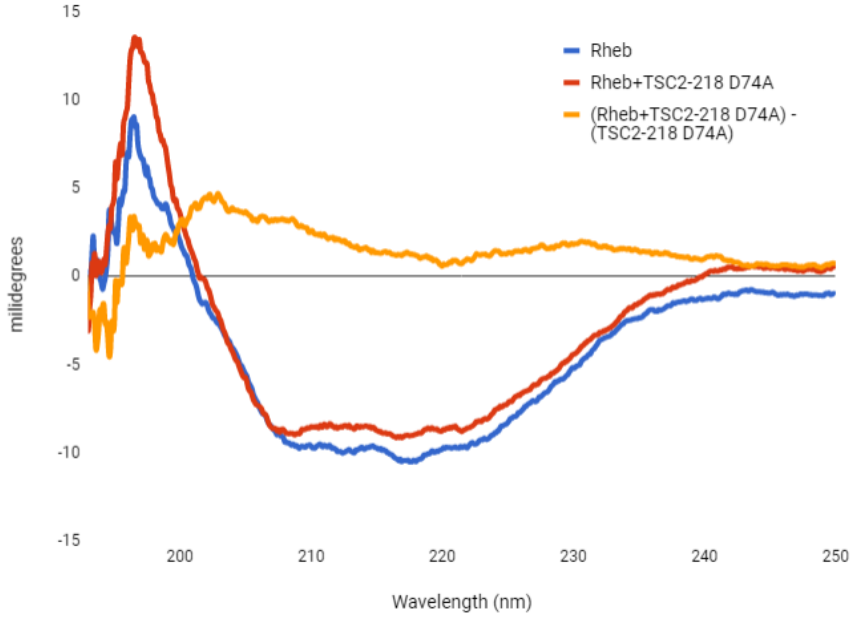

Figure 11B: Circular dichroism (CD) difference spectral data for Rheb in the presence and absence of TSC2-218 variant (D74A) was obtained using Jasco Spectra Measurement program. The data for wavelength vs CD intensity (millidegrees) of Rheb, TSC2-218 (D74A) and Rheb incubated with TSC2-218 (D74A) for 30min was exported and graphically presented using Excel. Corrected Rheb CD spectra was obtained similarly to the Rheb + WT sample.

3.2.2 GTPase Hydrolysis Assay

Intrinsic GTPase activity assays are performed to observe a protein's ability to undergo hydrolysis of GTP to GDP without the aid of any effectors. To determine the extent of intrinsic Rheb GTPase activity, various concentrations of Rheb was incubated with 10uM GTP (without any TSC2-218 GAP proteins) for 90 min and luminescence was measured. According to Figure 12, as the concentration of Rheb increased, the luminescence decreased. However, there was very little difference between luminescence (which corresponds to the GTP concentration) at 4uM and 0uM Rheb (Figure12).

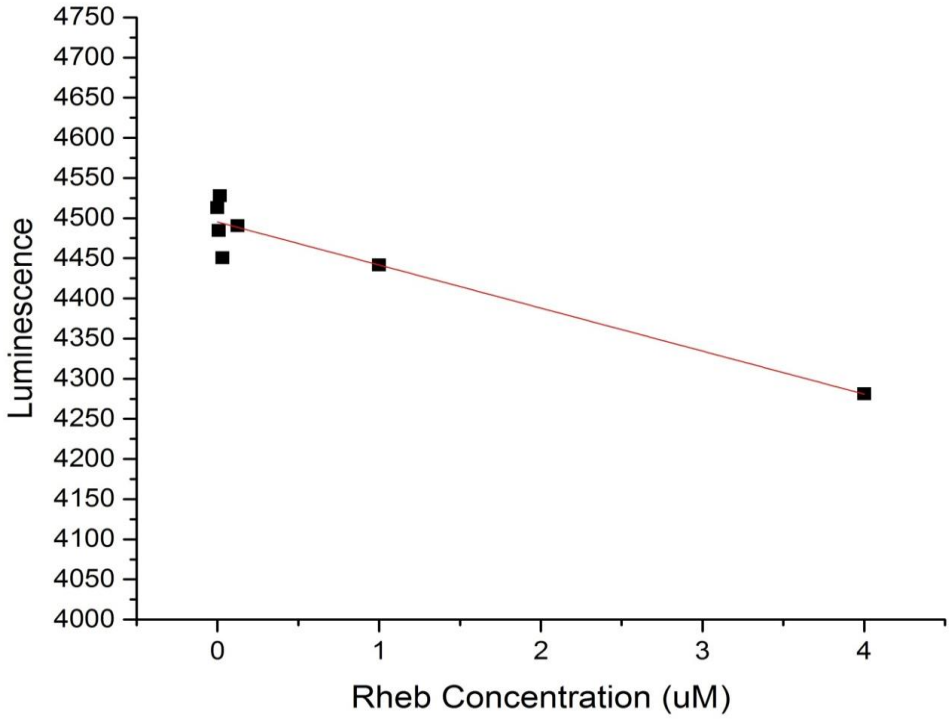

Figure 12. Graphical representation of intrinsic Rheb GTPase activity. Luminescence corresponds to the GTP concentration. Data was obtained using the Gen 5 program from BioTek and exported to Excel. The data was then plotted and fitted using Origin.

TSC2-218 WT and variant (D74A) were incubated with Rheb and GTP for 90min and then the luminescence was measured in order to observe the GAP effect of TSC2-218 WT and D74A on GTPase activity of Rheb. Figure 13 depicts that both Rheb + TSC2-218 WT group and

Rheb + TSC2-218 D74A group had lower GTP concentration than Rheb and GTP only. In addition, Rheb + D74A group showed a slightly lower GTP concentration than Rheb + WT (Figure 13).

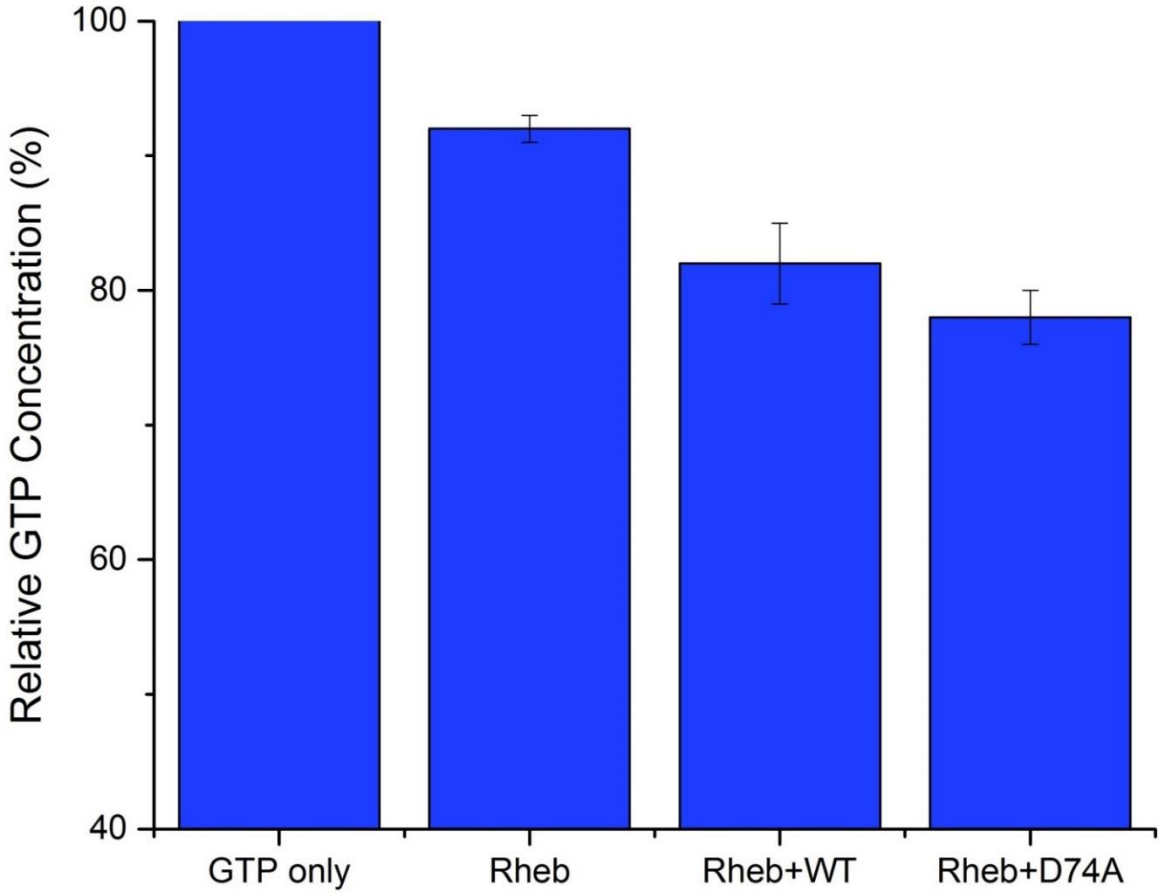

Figure 13. Graphical representation of GAP (TSC2-218 WT and D74A) stimulated Rheb GTPase activity. GTP only and Rheb only were used as controls. Data was obtained using the Gen 5 program from BioTek and exported to Excel. The data was then plotted and fitted using Origin.

To observe the effect of TSC2-218 WT and D74A concentration on GTPase activity of Rheb, increasing concentrations of TSC2-218 WT and variant (D74A) were incubated with Rheb and GTP for 90min and then the luminescence was measured. Figure 14 depicts that with increasing wild-type TSC2-218 and D74A concentration, GTP concentration was lowered. In

addition, the WT and variant GAP proteins displayed very little difference between relative GTP concentrations at each concentration (Figure 14).

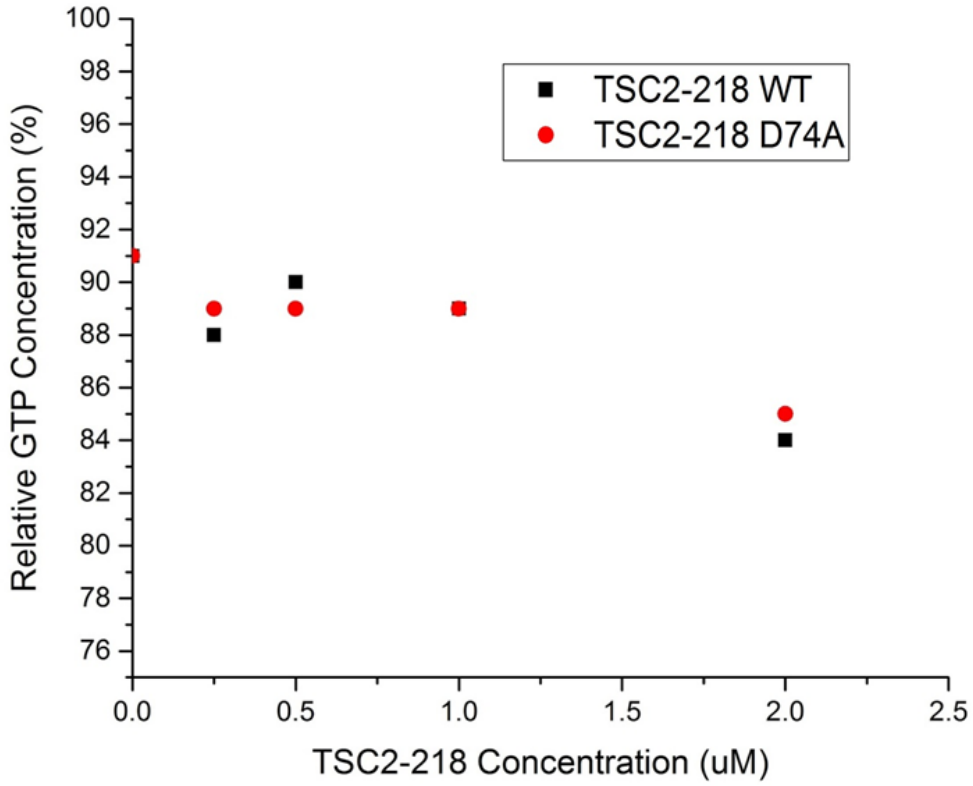

Figure 14. Graphical representation of GAP concentration-dependent study of Rheb GTPase activity in the presence of WT and variant, D74A. GTP only was used to normalize the luminescence data for all samples. Data was obtained using the Gen 5 program from BioTek and exported to Excel. The data was then plotted and fitted using Origin.

IV. Chapter 4: Conclusions and Future Directions

Ras superfamily GTPases are vital in regulating cell signaling and homeostasis. Rheb, the model Ras GTPase protein studied, signals the activation of the mTOR pathway that further activates cell division and growth. Due to its low intrinsic GTPase activity of Rheb, TSC2, a GAP protein, is needed to enhance Rheb GTP hydrolysis. Mutations in key residues in Rheb and TSC2 have been shown to disrupt the binding to, stability of, and/or enzyme activity of Rheb, leading to over stimulation of the mTOR pathway. In addition, the molecular details of the TSC2 interaction with Rheb are not completely understood. Therefore, a more comprehensive

investigation of the effect of single point mutations in residues of TSC2 that are homologous to key Ran1GAP residues, may shed more light on the Rheb-TSC2 interactions. This project focused on the single point mutation, D74A, in the region adjacent to the GAP catalytic region of TSC2 to examine the stabilization and binding effect of this reside on Rheb and TSC2. The homologous residue in Ran1GAP showed a decrease in GAP activity and resulted in down-regulation of GTPase activity in Ran1GTPase. Since this was not observed in TSC2, it was hypothesized that D74A could lead to stability of the TSC2-Rheb interaction and induce a more stable binding. Several experiments were performed to observe the structural stability of D74A, as well as, the interaction Rheb.

4.1 Characterization Studies of TSC2-218 (WT) and TSC2-218 (D74A)

According to the circular dichroism spectra, the mutation D74A showed comparable secondary structure, specifically alpha-helices, compared to the wild-type. Therefore, the single point mutation from aspartic acid to alanine helped in maintaining the protein in primarily an alpha helical form with minimal alternations to secondary structure.

Stability experiments were performed to observe any effect to the protein stability in the presence of chemical (urea) and thermal denaturants. The urea denaturation studies showed minimal difference in C_m between wild type (3.47M urea) and mutant (3.58M urea). The low difference of 0.11M urea between the wild type and variant suggests that the single point mutation does not disrupt the stability of the protein in the presence of a chemical denaturant (urea).

Thermal denaturation studies were performed to confirm the effect of the single mutation to the protein stability by increasing the temperature of the protein sample. According to the data derived from thermal denaturation studies, there is very little difference between the T_m values

for wild type (69.55°C) and D74A (70.80°C). This corresponds with the findings from the urea denaturation studies in that the single point mutation does not affect the stability of the protein.

Ultimately, the variant seems to have minimal effect on the secondary structure (primarily that of alpha helices) and the chemical and thermal protein stability of TSC2-218 overall, remained quite stable (maybe even slightly more stable) compared to that of the WT.

4.2 Interaction Studies between RHEB and TSC2-218 (WT and D74A)

The circular dichroism (CD) difference spectra showed that there was difference between the Rheb spectra and the mathematically calculated spectra of TSC2-218 mixture - TSC2-218 for both the TSC2-218 WT and D74A samples. This finding implicates that there is binding between the variant, D74A, and Rheb as the difference in spectra is caused by the conformational change upon TSC2-218 and Rheb due to binding.

The GTPase activity assay of Rheb in the presence of only 10uM GTP, suggested little difference in luminescence (which corresponds to GTP concentration) between high (4uM) and low (0uM) concentrations of Rheb (Figure 12). This data confirms the previous findings that the intrinsic GTPase properties of Rheb were very low.

When Rheb was incubated with TSC2-218 WT and D74A, both GAP proteins showed a distinct decrease in GTP concentration in comparison to Rheb only group and GTP only group (Figure 13). In addition, there was no large difference between the WT and variant TSC2-218 samples, which confirms that the single point mutation does not diminish its GAP activity towards Rheb and thus, Rheb GTPase activity is maintained. Further, in the TSC2-218 concentration dependent GTPase activity study, it was confirmed that TSC2-218 wild-type and D74A both enhanced GTP hydrolysis in Rheb and there was little difference between the WT

and variant in GAP activity. However, the assay would have to be performed with higher concentrations of TSC-218 in order to significantly confirm presence of any differences.

Characterization studies of the interaction between Rheb and TSC2-218 (D74A) have shown that the mutation does not seem to diminish the overall ability to bind to Rheb (seen by the maintained difference in difference CD spectra) or GAP activity towards Rheb.

4.3 Future Directions

In conclusion, this project has detailed preliminary information of TSC2-218 (D74A) in terms of stability, secondary structure, GAP stimulated Rheb GTPase activity and qualitative binding interactions with Rheb. This information can also be used to draw conclusions on overall interactions between Rheb-TSC2. In addition, it is an unique TS2 residue that is able to stabilize the interaction with Rheb in comparison to similar mutations in homologous GAP proteins. However, more work needs to be done to understand the molecular details of Rheb-TSC2 binding.

Since there is limited information on the structure of TSC2, it would be interesting to study TSC2 WT and variants using NMR (nuclear magnetic resonance) and/or X-Ray crystallography. Though previous attempts have been made to employ NMR to study TSC2, obstacles, such as the propensity of TSC2 to aggregate at high concentrations (necessary for NMR), have made it difficult to obtain viable data (39). Further attempts need to be made to optimize conditions to enable NMR characterization. Alternatively, X-Ray crystallography can also be used to derive structural information on wild-type and variant TSC2.

Further, one of the main goals of studying D74A single mutation is to observe binding with Rheb. Since GAP activity is maintained in the variant, it is important to examine the binding capacity of D74A in relation to wild-type. This can be done by performing in-vitro

binding assays and isothermal titration calorimetry (ITC). In-vitro binding can be performed using affinity chromatography and SDS-PAGE and provides qualitative information about TSC2-Rheb binding. In contrast, ITC provides quantitative thermodynamic binding data.

A more comprehensive study of TSC2, wild-type and variant, and molecular details of its interaction with Rheb is vital to understanding specific role of D74A in TSC2 and why it does not follow the trend of its Ran1GAP homolog. In addition, these findings will also aid in shedding light on the specific key residues and general interaction of TSC2 and Rheb. These results can also be applied to Ras proteins and their effectors as a whole. Furthermore, conclusions from these studies may be used to optimize drug treatments for tuberous sclerosis diseases by shedding light on possible targeting sites.

REFERENCES

1. Bourne, H., Sanders, D. and McCormick, F. (1990). The GTPase superfamily: a conserved switch for diverse cell functions. *Nature*, 348(6297), pp.125-132.

2. Carroll B, Maetzel D, Maddocks OD, et al. Control of TSC2-Rheb signaling axis by arginine regulates mTORC1 activity. Mizushima N, ed. *eLife*. 2016;5:e11058. doi:10.7554/eLife.11058.

3. Cargnello M, Tcherkezian J, Roux PP. The expanding role of mTOR in cancer cell growth and proliferation. *Mutagenesis*. 2015;30(2):169-176. doi:10.1093/mutage/geu045.

4. Jacinto E, Loewith R, Schmidt A, Lin S, Rüegg MA, Hall A, Hall MN. (2004) Mammalian TOR complex 2 controls the actin cytoskeleton and is rapamycin insensitive. Nat Cell Biol6:1122–1128.

5. D. D. Sarbassov, Siraj M. Ali, Do-Hyung Kim, David A. Guertin, Robert R. Latek, Hediye Erdjument-Bromage, Paul Tempst, David M. Sabatini. Rictor, a novel binding partner of mTOR, defines a rapamycin-insensitive and raptor-independent pathway that regulates the cytoskeleton. Curr Biol. 2004 Jul 27; 14(14): 1296–1302. doi: 10.1016/j.cub.2004.06.054

6. Laplante M, Sabatini DM. mTOR signaling in growth control and disease. *Cell*. 2012;149(2):274-293. doi:10.1016/j.cell.2012.03.017.

7. Sato T, Nakashima A, Guo L, Tamanoi F. Specific Activation of mTORC1 by Rheb G-protein *in Vitro* Involves Enhanced Recruitment of Its Substrate Protein. *The Journal of Biological Chemistry*. 2009;284(19):12783-12791. doi:10.1074/jbc.M809207200.

8. Qian Yang, Ken Inoki, Eunjung Kim, Kun-Liang Guan. TSC1/TSC2 and Rheb have different effects on TORC1 and TORC2 activity. Proceedings of the National Academy of Sciences May 2006, 103 (18) 6811-6816; DOI:10.1073/pnas.0602282103

9. Efeyan A, Sabatini DM. mTOR and cancer: many loops in one pathway. *Current opinion in cell biology*. 2010;22(2):169-176. doi:10.1016/j.ceb.2009.10.007.

10. Jia G, Aroor AR, Martinez-Lemus LA, Sowers JR. Overnutrition, mTOR signaling, and cardiovascular diseases. *American Journal of Physiology - Regulatory, Integrative and Comparative Physiology*. 2014;307(10):R1198-R1206. doi:10.1152/ajpregu.00262.2014.

11. Yamagata K, Sanders LK, Kaufmann WE, Yee W, Barnes CA, Nathans D, Worley PF. 1994. rheb, a growth factor- and synaptic activity-regulated gene, encodes a novel Ras-related protein. J Biol Chem 269:16333–16339.

12. Yu Y, Li S, Xu X, et al. Structural basis for the unique biological function of small GTPase RHEB. *J Biol Chem*. 2005;280(17):17093-17100. doi:10.1074/jbc.M501253200

13. F. McCormick, B. F. Clark, T. F. la Cour, M. Kjeldgaard, L. Norskov-Lauritsen, J. Nyborg. A model for the tertiary structure of p21, the product of the ras oncogene. Science. 1985 Oct 4; 230(4721): 78–82.

14. I. R. Vetter, A. Wittinghofer.The guanine nucleotide-binding switch in three dimensions. Science. 2001 Nov 9; 294(5545): 1299–1304. doi: 10.1126/science.1062023

15. Wittinghofer, A. (1999) in *GTPase* (Hall, A., ed) Oxford University Press, Oxford

16. Karassek S, Berghaus C, Schwarten M, et al. Ras homolog enriched in brain (Rheb) enhances apoptotic signaling. *J Biol Chem*. 2010. doi:10.1074/jbc.M109.095968.

17. Jurnak, F. (1985) Structure of the GDP domain of EF-Tu and location of the amino acids homologous to ras oncogene proteins, Science 230, 32-36.

18. Brendan D. Manning, Lewis C. Cantley. Rheb fills a GAP between TSC and TOR. Trends Biochem Sci. 2003 Nov; 28(11): 573–576. doi: 10.1016/j.tibs.2003.09.003

19. Edward Im, Friederike C. von Lintig, Jeffrey Chen, Shunhui Zhuang, Wansong Qui, Shoaib Chowdhury, Paul F. Worley, Gerry R. Boss, Renate B. Pilz. Rheb is in a high activation state and inhibits B-Raf kinase in mammalian cells. Oncogene. 2002 Sep 12; 21(41): 6356–6365. doi: 10.1038/sj.onc.1205792

20. Garami A, et al. Insulin activation of Rheb, a mediator of mTOR/S6K/4E-BP signaling, is inhibited by TSC1 and 2. Mol. Cell. 2003;11:1457–1466. doi: 10.1016/S1097-2765(03)00220-X

21. Tee AR, Manning BD, Roux PP, Cantley LC, Blenis J. 2003. Tuberous sclerosis complex gene products, Tuberin and Hamartin, control mTOR signaling by acting as a GTPase-activating protein complex toward Rheb. Curr Biol 13:1259–1268. doi:10.1016/S0960-9822(03)00506-2.

22. Inoki K, Li Y, Xu T, Guan K-L. Rheb GTPase is a direct target of TSC2 GAP activity and regulates mTOR signaling. *Genes & Development*. 2003;17(15):1829-1834. doi:10.1101/gad.1110003.

23. Zhang Y, et al. Rheb is a direct target of the tuberous sclerosis tumour suppressor proteins. Nat. Cell Biol. 2003;5:578–581. doi: 10.1038/ncb999.

24. Castro AF, Rebhun JF, Clark GJ, Quilliam LA. Rheb binds tuberous sclerosis complex 2 (tsc2) and promotes s6 kinase activation in a rapamycin-and farnesylation-dependent manner. Journal of Biological Chemistry. 2003;278:32493–32496. doi: 10.1074/jbc.C300226200.

25. Aspuria, P. J., and Tamanoi, F. (2004) The Rheb family of GTP-binding proteins, Cellular signalling 16, 1105-1112.

26. Lee, C. H., Inoki, K., and Guan, K. L. (2007) mTOR pathway as a target in tissue hypertrophy, Annu Rev Pharmacol Toxicol 47, 443-467.

27. Zhang Y, et al. Rheb is a direct target of the tuberous sclerosis tumour suppressor proteins. Nat. Cell Biol. 2003;5:578–581. doi: 10.1038/ncb999.

28. Scrima A, Thomas C, Deaconescu D, Wittinghofer A. The Rap–RapGAP complex: GTP hydrolysis without catalytic glutamine and arginine residues. *The EMBO Journal*. 2008;27(7):1145-1153. doi:10.1038/emboj.2008.30.

29. Narayanan V. Tuberous sclerosis complex: genetics to pathogenesis. *Pediatric Neurology*. 2003;29(5):404–409. doi: 10.1016/j.pediatrneurol.2003.09.002.

30. Plank TL, Logginidou H, Klein-Szanto A, Henske EP. The expression of hamartin, the product of the TSC1 gene, in normal human tissues and in TSC1- and TSC2-linked angiomyolipomas. *Mod Pathol*. 1999.

31. MM Maheshwar, R Sandford, M Nellist, JP Cheadle, B Sgotto, M Vaudin, JR Sampson. Comparative analysis and genomic structure of the tuberous sclerosis 2 (TSC2) gene in human and pufferfish Hum Mol Genet, 5 (1996), pp. 131-137

32. Li, Y., Inoki, K., and Guan, K. L. (2004) Biochemical and functional characterizations of small GTPase Rheb and TSC2 GAP activity, Molecular and cellular biology 24, 7965-7975.

33. Marshall CB, Ho J, Buerger C, Plevin MJ, Li G-Y, Li Z, Ikura M, Stambolic V. Characterization of the intrinsic and TSC2-GAP-regulated GTPase activity of Rheb by real-time NMR. Sci Signal. 2009;2(55):ra3. doi: 10.1126/scisignal.2000029.

34. S. Tayyab, M.U. Siddiqui, N. Ahmad. Experimental determination of the free energy of unfolding of proteins Biochem. Ed., 23 (1995), pp. 162-164

35. Roy A, Kucukural A, Zhang Y. I-TASSER: a unified platform for automated protein structure and function prediction. *Nature protocols*. 2010;5(4):725-738. doi:10.1038/nprot.2010.5.

36. Zhang Y. I-TASSER server for protein 3D structure prediction. *BMC Bioinformatics*. 2008;9:40. doi:10.1186/1471-2105-9-40.

37. PDB ID 1XTS.pdb

    Yu Y, Li S, Xu X, et al. Structural basis for the unique biological function of small GTPase RHEB. *J Biol Chem*. 2005;280(17):17093-17100. doi:10.1074/jbc.M501253200 PDB ID

38. PDB ID 1XTQ.pdb

    Yu Y, Li S, Xu X, et al. Structural basis for the unique biological function of small GTPase RHEB. *J Biol Chem*. 2005;280(17):17093-17100. doi:10.1074/jbc.M501253200 PDB ID

39. Morris, Kyla Marie Morinini, "Biochemical and Biophysical Studies of Novel Features of Ras-related Protein Interactions" (2013). *Theses and Dissertations*. 1002.